

Abstract

6.1 Introduction

6.2 Materials and Methods

6.3 Results

6.4 Discussion

6.5 Conclusion

6.6 References

Abstract

Traditional knowledge based medicines have gained worldwide attention and presently the scientific community is focusing on proper pharmacological validation and identification of lead compounds for the treatment of various diseases. The South East region of India is the home of valuable traditional herbal remedies. *Calotropis gigantea* is one such medicinal plant used by traditional healers for the treatment of various disorders. The present study was aimed to evaluate the anticancer activity of ethanol (EECGL) and water (WECGL) extracts of *Calotropis gigantean* latex against Dalton's Ascitic Lymphoma (DLA) cells in *in vitro* and *in vivo* experimental conditions. The extracts inhibit the proliferation of DLA cells in a dose-dependent manner. Studies on cell viability, chromatin condensation using DAPI and PI staining and DNA fragmentation revealed that *C.gigantea* latex extracts were capable to produce significant anticancer and apoptotic effects on DLA cells. Studies on cellular redox balance, nitric oxide release level, reactive oxygen species formation and alteration of mitochondrial membrane potential confirmed the oxidative injury in DLA cells by *C.gigantea* latex extracts. In cell cycle study, the latex extracts induced apoptosis in DLA cells and there was significant cell cycle arrest at the G₀/G₁ phase. To show the abilities in cancer chemoprevention, *in vivo* studies were also done in DLA-bearing Swiss albino mice. Significant reduction in body weight, tumour volume and viable tumour cell count and increase in mean survival time were observed. Surprisingly EECGL and WECGL had no toxic effects on normal lymphocytes at doses up to 50 µg ml⁻¹. The results of this investigation clearly demonstrate that the latex extracts of *Calotropis gigantea* inhibit the cell proliferation

and survival of DLA cells via oxidative injury and induction of apoptosis in a dose-dependent manner.

Saswata Sanyal, Pralay Maity, Ananya Pradhan, Madhubanti Bepari, Surya Kanta Dey, Sujata Maiti Choudhury*. *Calotropis gigantea latex* exhibits antioxidant potential in Dalton's ascites lymphoma (DLA) bearing mice. *World Journal of Pharmaceutical Research*. 2016; 5:1617-1632.

6.1 Introduction

The medicinal plants serve primary role in the preservation of health as well as prevention and management of many diseases including cancer. Today they have become a subject of intense research. The world Health Organization has also recognized the role of traditional systems of medicine, which depend largely upon the medicinal plants to achieve its goal "Health for all by 2020" (Yoganarasimhan, 1996).

Lymphoma and its treatments

Every year thousands of individuals are affected by lymphoma. Lymphoma is a cancer of the lymph system. The lymph system is an interconnected network of thin tubes and nodes that carries white blood cells. These cells fight infections and are vitally important for our well-being. So when a lymphocyte that is a part of the lymph system becomes cancerous, it may grow and multiply to form a lymphoma. Lymphoma may affect any of the parts of the lymph system. In fact, lymphomas can occur in other organs such as lymph nodes, spleen, bone

marrow etc. There are two main types of lymphoma - Hodgkins lymphoma (HL) and Non-Hodgkin Lymphoma (NHL) (Malik, 2007).

T cell lymphomas are a type malignancy of the immune system that affects 15,884 per 100,000 males and 7,918 per 100,000 females in India. The rate of mortality among males for NHL was 11,071 per 100,000 and 5,526 per 100,000 for females (State of Healthcare in India - Lymphoma Coalition, 2015). The more common NHLs (approx 90% of all lymphomas) can be further divided into B- and T-cell lymphomas depending on the cell type of origin. T-cell lymphomas are clonal tumours of immature or mature T lymphocytes at various stages of differentiation. They account for only 10-12% of all NHLs, the rest being of B-cell origin. The clinical appearance of lymphomas is often a swollen lymph node in the neck, axilla, but several other are common such as abdominal or mediastinal masses or extra nodal indices. Several patients have general symptoms at time of diagnosis such as weight loss, fever and sweating. Most of the patients with newly diagnosed lymphoma require immediate treatment, but some forms of lymphoma have an indolent course and treatment can be postponed for several years after diagnosis. Standard treatment for lymphomas in need of treatment is combination chemotherapy in repeated cycles. For B-cell lymphomas, the addition of an anti-CD20 antibody has improved outcome substantially and is now a part of the standard treatment. T-cell lymphomas are generally associated with inferior outcome than lymphomas of B-cell origin (Gisselbrecht et al., 1998), and continuous effort is put into finding new treatment modalities or efficient combinations of existing treatments. Addition of an anti-CD52 antibody and high-dose chemotherapy with stem cell rescue are currently being tested

in clinical trials. Radiation therapy is also important in lymphoma treatment, both with curative and comforting intention (Li et al., 2006). T-cell lymphomas resemble stages of normal T-cell differentiation and some of them can be classified according to the corresponding normal stage. However, for some of the lymphomas the normal counterpart is not yet identified (Swerdlow et al., 2008). The cells of the adaptive immune system are T and B lymphocytes, allow highly specific and strong response to pathogen. Gross examination from different literature it is revealed that the mice affected by the disease showed enlargement of lymph nodes, spleen, liver, thymus and kidneys. Histopathologic analysis showed in different literature: tumors to be of lymphoid origin with the morphological appearance of medium sized monotonous lymphoblast (Coustan-Smith et al., 2009).

Dalton's ascites lymphoma and the role of medicinal plants

Dalton's lymphoma ascites (DLA) has become an imperative tool in cancer research. Several studies have been designed using DLA as a model of *invivo* and *invitro* cancer study. Methanol extract of *Cissampelos pariera* (MECP) was reported to show a potent cytotoxic activity against DLA cells and caused a significant decrease in packed cell volume, viable cell count, and an increase in lifespan in DLA-bearing mice. The altered haematological and serum biochemical profiles and antioxidant enzymes were restored to normal levels in MECP-treated mice (Samuel et al., 2014). Ethanolic and aqueous extracts of *Vitex negundo* Linn. Leaf were also reported to have antitumor efficacy against DLA cells (Dewade et al., 2010). Ethanolic extract of *Dendrobium formosum* caused apoptosis and arrested the

DLA cell cycle at G₂/M phase (Prasad and Koch, 2014). Different doses of ethanolic extract of *Cnidioscolus chayamans* decreased the average increase in body weight, reduced the packed cell volume (PCV), viable tumor cell count and increased the life span of DLA treated mice and brought back the haematological parameters, serum enzyme and lipid profile near to normal values (Kulathuranpillai et al., 2012). The ethanolic root extract of *L. inermis* reversed the increased number of WBC count, platelets and lymphocytes and decreased number of RBC count, haemoglobin content and monocytes (Priya et al., 2011).

The selective anti-proliferative activity of *Calotropis* species is of high interest as an anticancer agent from herbal origin because the species exhibits several pharmacological activities which are used in traditional treatment (Habib and Karim, 2013). Till now very little is known regarding the anticancer activity of plant latex as well as its specific mechanism of action on T-cell lymphomas. Due to this in the present study, attempts were made to evaluate the antitumor and as well as cytotoxic, apoptotic potential of ethanol (EECGL) and water (WECGL) extract of *Calotropis gigantea* latex against Dalton's ascites lymphoma (DLA) cells in *invitro and invivo* experimental conditions.

6.2. Materials and methods

6.2.1. Chemicals and reagents

RPMI 1640, penicillin and streptomycin were purchased from Sigma Aldrich Co, LLC, US. Fetal bovine serum (FBS) was purchased from GIBCO. 3-(4,5-dimethyl-2-thiazolyl)- 2,5-diphenyl-tetrazolium bromide (MTT), Dimethyl sulfoxide (DMSO), Histopaque-1077,

sodium dodecyl sulphate (SDS), 2',7'-Dichlorodihydrofluorescein diacetate (H2DCFDA), propidium iodide (PI), 4',6'-diamidino-2-phenylindole (DAPI), Rhodamine 123, 5-fluorouracil, 5,5-Dithiobis-(2-nitrobenzoic acid) (DTNB), Tris-HCl, Tris buffer, Titron X-100, phenol, chloroform, iso-amyl alcohol, ethidium bromide (EtBr), Acridine orange (AO), 2-vinylpyridine, Ethylenediaminetetraacetic acid (EDTA), Tricarboxylic acid (TCA), and other chemicals were purchased from Sigma-Aldrich, St. Louis, MO, USA; Himedia India, Ltd., Mumbai, India; and Merck India, Ltd., Mumbai, India for the experimentation.

6.2.2. Animals

Adult male Swiss albino mice weighing 22-25 g were used for the maintenance of Dalton ascites lymphoma (DLA) cell line and for the *in vivo* tumour regression study. The mice were housed in poly acrylic cage (38x 23x10 cm). The animals were kept on a 12 h light: 12 h dark regime at 25 °C for 7 days before commencement of the experiment. The animals had free access to standard diet and water. Mice were deprived of food but not water prior to administration of the test extracts. The study was approved by the Institutional Animal Ethical Committee (IAEC), registered under Committee for the Purpose of Control and Supervision of Experiments on Animals (CPCSEA), Ministry of Environment, Forests & Climate Change, and Govt. of India and performed in compliance with the relevant laws and guidelines of the CPCSEA.

6.2.3. Cell lines

Dalton ascites lymphoma (DLA) cells were obtained from Chittaranjan National Cancer Research Institute (CNCR), Kolkata. DLA cells were maintained by weekly intraperitoneal transplantation in the male albino Swiss mice at the concentration of 1×10^6 /cells per mouse. Washed DLA cells free from contaminating RBC were cultured in RPMI-1640 medium supplemented with 10% fetal bovine serum (FBS) and antibiotic antimycotic solution (100 U ml⁻¹ penicillin, 10 mg ml⁻¹ streptomycin and 4 mM L-glutamine) under 5% CO₂ and 95% humidified atmosphere at 37°C in an incubator. Viable cells (1×10^6 ml⁻¹) were used for different experiments in the present study.

6.2.4 Isolation of mice lymphocyte cell (MLC)

Blood samples were collected from the healthy male mice for the separation of lymphocytes. The lymphocytes were isolated from heparinised blood samples according to the method of Hudson and Hay (Hudson and Hay, 1989). About 2 ml of blood were layered onto same amount of Histopaque 1077 (Sigma-Aldrich Co. LLC., US) and centrifuged at 2000 rpm for 30 min at room temperature. The upper buffy coat layer containing lymphocytes was transferred to a clean centrifuge tube and washed three times in balanced salt solution (PBS). The mice lymphocytes (MLCs) were resuspended in RPMI complete media supplemented with 10% FBS and incubated for 24 h at 37 °C in a 95% humidified and 5% CO₂ atmosphere in a CO₂ incubator.

6.2.5 *In-vitro* study

6.2.5.1 Experimental design for *in-vitro* study

Dalton ascites lymphoma (DLA) (1×10^6 cells) cells were exposed to different concentrations (5, 10, 25 and 50 $\mu\text{g ml}^{-1}$) of EECGL and WECGL for 24 h. Control cells did not receive any extract treatment. After the treatment schedule, the cells were collected separately and centrifuged at 1000–1200 rpm for 5 min at 4°C to separate cells and supernatants. The cells were washed with PBS (pH-7.4). A required amount of cells was lysed and then processed for biochemical estimation.

6.2.5.2 *In-vitro* cell viability assay

MLC, DLA cells were maintained in RPMI-1640 supplemented with 10% FBS, penicillin (100 U ml^{-1}), and streptomycin (10 mg ml^{-1}) in a humidified atmosphere of 5% CO_2 at 37°C . The cytotoxicity of EECGL and WECGL on MLC and DLA cells was determined by the MTT assay. Cells (1×10^6 per well) were plated in 100 μl of medium per well in 96 well plates and then the cells were incubated after the treatment of EECGL and WECGL for 24 h at 37°C . After removal of the treated compound the cells were washed with PBS (pH 7.4) and 5 mg ml^{-1} of 0.5% MTT in phosphate-buffered saline solution were added in each well. After 3

h of incubation, 0.1% DMSO was added to each well. The optical density (OD) was measured (Mosmann, 1983) at 540 nm on ELISA ANALYSER (Bio-Rad, Model 680). All experiments were performed in triplicate manner, and the effect on the proliferation of DLA cells was expressed as the % of cell viability.

6.2.5.3 Estimation of reduced glutathione (GSH)

At first, each sample (0.2 ml) was mixed with 4% sulfosalicylic acid and centrifuged at 2000 rpm for 10 min to settle the precipitated proteins. In aspirated supernatant 2 ml of 0.6 mM DTNB was added. Then the optical density of the yellow-colored complex formed by the reaction of GSH and DTNB was measured at 412-420 nm (Griffith, 1981).

6.2.5.4 Intracellular Reactive oxygen species (ROS) measurement (Roy et al., 2008)

The method has been discussed in chapter-3.

6.2.5.5 Nitric oxide release and generation assay

After the treatment schedule, 100 μl of Griess reagent (containing 1 part of 1% sulfanilamide in 5% phosphoric acid, and 1 part of 0.1% of N-C-1 naphthyl ethylene diamine dihydrochloride) (Merck-Millipore, India) was added to 100 μl of sup and incubated at room temperature for 10 min; readings were taken in a UV spectrophotometer at 550 nm (Chakroborty et al., 2011) and compared with a sodium nitrite standard curve (values ranging from 0.5 to 25 μM). The levels of NO were expressed as μMmg^{-1} protein.

6.2.5.6 Lactate dehydrogenase release assay

The treated cells were incubated for 18 h, after which 40 μl of the medium was transferred to 96-well plate to determine LDH release (Al-Qubaisi et al., 2011). Then 6% triton X-100 was added to the 96-well plates to determine the total LDH concentration. An aliquot of 4.6 mM pyruvic acid in potassium phosphate buffer (pH 7.5) was added to each well of the plate containing the medium followed by 100 μl of 0.4 mgml^{-1} reduced β -NADH in 0.1 M potassium phosphate buffer (pH 7.5). The kinetic change in absorbance was read at 340 nm for 1 min in an ELISA microplate reader (Bio-Rad, Model 680).

6.2.5.7 Cellular morphology study by polarizing microscopy

DLA cells were treated with EECGL and WECGL in RPMI media for 24h. After incubation blebbing of cell membranes were observed under polarizing microscope (Roy et al., 2008).

6.2.5.8 Chromatin condensation by PI and DAPI staining

DLA cells (1×10^6 cells ml^{-1}) were seeded in petriplate and incubated with EECGL and WECGL for 24h at 37°C and 5% CO_2 . The cells were then fixed by 70% ethanol and incubated at -20°C for 2 hours. After fixation, cells were washed and stained with DAPI ($1 \mu\text{g ml}^{-1}$) at 37°C for 5 minutes and RNase-propidium iodide (PI) mixture (1mg ml^{-1}) at 37°C for 15 minutes. The cells were washed with phosphate buffer and observed under fluorescence microscope (LEICA DCF295, Germany) (Prasad and Koch, 2014).

6.2.5.9 Acridine orange–ethidium bromide staining

A number of 1×10^6 DLA cells were seeded into each well plate and incubated for 24 h at 37°C in a humidified 5% CO_2 atmosphere. EECGL and WECGL were then added to the well for 24 h. After incubation, cells were washed with PBS buffer. Then on a clean glass slide 10 μl of washed cells were placed and 10 μl each of acridine orange ($50 \mu\text{g ml}^{-1}$) and ethidium bromide ($50 \mu\text{g ml}^{-1}$) were mixed (Ho et al., 2009). Then cells were observed under a fluorescence microscope (LEICA DCF295, Germany).

6.2.5.10 DNA fragmentation study by agarose gel electrophoresis (Gong et al., 1994)

The method has been discussed in chapter-5.

6.2.5.11 Measurement of Mitochondrial membrane potential by Rhodamine 123

In brief, DLA cells were treated with EECGL and WECGL for 24 h. After treatment, cells were washed with culture media followed by incubation with 1.5 μ M Rhodamine 123 for 15 min at 37°C in a humidified chamber. The cells were then washed and the fluorescence intensity of rhodamine 123 was monitored for 2 min using a fluorescence spectrophotometer. An aliquot of cell suspension was also used for microscopic observations (LEICA DCF295, Germany). The cellular mitochondrial membrane potential was expressed as a percentage of control cells at an excitation wavelength of 493 nm and an emission wavelength of 522 nm (M'Bemba-Meka et al., 2006).

6.2.5.12 Study of DNA fragmentation by alkaline comet assay

DNA fragmentation was further assessed by alkaline comet assay with few modifications. Briefly, DLA cells were treated with EECGL and WECGL at IC₅₀ doses for 24 h. After treatment, cells were washed with phosphate buffer. Then the cell pellet was mixed with 0.7% agarose for performing the comet assay. The glass slide was smeared with 1% agarose and covered with cell pellet. Then slides were poured in lysis buffer and electrophorized. Then the slides were stained with fluorescence stain ethidium bromide and image was

captured under fluorescence microscope (LEICA DFC295, Germany). The comet tail length was calculated as the distance between the end of heads and end of each tail. Tail moments were defined as the product of the percentage of DNA in each tail and % DNA (tail) presented as: $TA \times TAI \times 100 / [(TA \times TAI) + (HA \times HAI)]$; whereas TA= tail area, TAI=tail area intensity, HA=head area and HAI=head area intensity (Alcantraet al.,2011). All measurements were done in triplicate manner.

6.2.5.13 Detection of cellular apoptosis by flow cytometry

Cell cycle study was done by flow cytometric analysis. Briefly, after EECGL and WECGL exposure for 24 h the cells were centrifuged at 1000-1200 rpm for 5 min. After washing, cells were resuspended in PBS. Cells were incubated with RNase (10 mg ml⁻¹) solution for 1 h at 37°C. After incubation, cells were stained at dark with propidium iodide (1 mg ml⁻¹) for 15 min at room temperature. Then cells were washed with PBS buffer and diluted with 500 ml of PBS. Then, the cell cycle was analyzed using flow cytometer (BD FACSVerse) (Nunez, 2001) and Cell Quest software.

6.2.6 In-vivo study

6.2.6.1 Treatment schedule

Seventy two male mice were divided into seven groups (n=11).

Group I : Saline control

Group II : DLA control

Group III : DLA + EECGL/ WECGL (100mg/kg body weight)

Group IV : DLA + EECGL/WECGL (200 mg/kg body weight)

Group V : DLA + 5-FU 20 mg/kg body weight

Except first group, all group animals were inoculated with 0.1 ml of 1×10^6 DLA cells/mouse intraperitoneally. The second group served as DLA control. After 24 h of tumour inoculation, III and IV groups received respective test extract once daily and the group V received reference drug 5-FU once daily for 14 consecutive days (Haldar et al., 2010). Twenty four hours after last dose and 18 h of fasting, blood was collected from six mice of each group for the estimation of haematological parameters. Then the animals were sacrificed by cervical dislocation, ascites fluid was drawn from peritoneal cavity for the study of tumor regression parameters (Gupta et al., 2007) and liver and kidney tissue was collected to perform and hepatic and renal oxidative stress parameters..

6.2.6.2 Change in Body weight

Tumor growth was monitored by daily body weight change from the day of zero to the day of sacrifice (Maiti Choudhury et al.,2010).

6.2.6.3 Studies on host survival time

The survival time of host mouse was assayed (Jacob and Latha,2013) by recording the mortality for 6 weeks using the following equations.

Mean survival time (MST) = (Day of first death + Day of last death)/2,

Increase life span (ILS) (%) = [(Mean survival time of treated group/mean survival time of control group) - 1] x 100

6.2.6.4 Tumor volume

At the time of sacrifice, 2ml of normal saline was injected in intraperitoneal cavity of each mice. Then mixture of tumor cells and saline were aspirated aseptically from the peritoneal cavity of mice and the tumor volume was calculated (Bala et al.,2010).

6.2.6.5 Tumor cell count

The ascitic fluid was taken in a WBC pipette and diluted 100 times with phosphate buffer saline. Then a drop of the diluted cell suspension was counted in Neubauer counting chamber (Saha et al.,2011).

6.2.6.6 Red (RBC) and white(WBC) blood cell count (Wintrobe,1967)

The method has been discussed in chapter-3.

6.2.6.7 Determination of haemoglobin (Dacie and Lewis, 1958)

This method has been described in chapter-3.

6.2.6.8 Estimation of malondialdehyde (MDA) content

MDA content of liver and kidney homogenate was measured by the method of Ohkawa. (Ohkawa et al., 1979). One ml homogenate (20 mg/ml phosphate buffer) was mixed with 0.2 ml of 8.1% sodium dodecyl sulfate, 1.5 ml of acetate buffer (20% pH 3.5), and 1.5 ml of aqueous solution of thiobarbituric acid (0.8%) were taken. After heating at 95°C for 60 min, the red pigment produced was extracted with 5 ml of *n*-butanol-pyridine mixture (15: 1) and centrifuged at 5000 rpm for 10 min at room temperature. The absorbance of supernatant was estimated at 535 nm.

6.2.6.9 Estimation of reduced glutathione (GSH)

Reduced glutathione was estimated by the method of Griffith. (Griffith, 1981). At first 100 µl sulfosalicylic acid was mixed with 200 µl homogenate and the mixture was centrifuged for 10 min at 3000 rpm. Then 1.8 ml of DTNB was added with the supernatant and was shaken well. Reading was taken at 412 nm.

6.2.6.10 Estimation of superoxide dismutase (SOD)

Superoxide dismutase of homogenate was measured by the method of Marklund and Marklund. (Marklund and Marklund, 1974). The SOD activity of the supernatant was estimated by measuring the percentage of inhibition of the pyrogallol autooxidation by SOD. The buffer contained 50 mM TrisHCl, 10 mM hydrochloric acid (HCl) in the presence of 1 mM EDTA. Then 2 ml of buffer mixture, 100 µl of 2 mM pyrogallol and 10 µl of

homogenate were poured in a spectrophotometric cuvette and the reading was measured in the spectrophotometer (UV-245 Shimadzu, Japan) at 420 nm for 3 min.

6.2.6.11 Estimation of catalase (CAT)

Catalase was estimated by the method of Aebi. (Aebi, 1974). After mixing of 1 ml of 30mM H_2O_2 and 1.9ml of 15mM PBS in 0.1ml of homogenate, readings were noted in the spectrophotometer at 240nm at 30 sec interval.

6.2.6.12 Estimation of glutathione peroxidase (GP_x)

Glutathione peroxidase was measured by the method of Rotruck et al. (Rotruck et al., 1973). Homogenate of liver and kidney (0.2 ml) was added with 0.1 ml of 2.5 mM H_2O_2 , 0.2 ml of 0.4 M sodium phosphate buffer, 0.1 ml of 10 mM sodium azide and 0.2 ml of 4 mM reduced glutathione and was incubated for 5 min at 37°C. Then 0.4 ml of 10% TCA was added to stop the reaction and centrifuged at 3200 rpm for 20 min. Then 1 ml of 5, 5'-dithiobisnitrobenzoic acid (DTNB) and 3 ml of di sodium hydrogen phosphate (Na_2HPO_4) were added to 0.5 ml of supernatant. The absorbance was measured at 420 nm.

6.2.6.13 Estimation of glutathione-s-transferase (GST)

Glutathione-S-transferase (GST) activity was estimated by the method of Habig. (Habig et al.,1974). Reaction mixture containing 0.1 ml of homogenate, 0.2 ml of 100 mM PBS, 0.05 ml of 1 mM GSH and 0.02 ml of 60mM 1-Chloro-2, 4 dinitrobenzene (CDNB) were taken in a cuvette and reading was noted at 340nm. The values were expressed in μmol CDNB conjugate formed/min/ mg protein.

6.2.7 Statistical analysis

All the parameters were performed in triplicate manner. The data was expressed as Mean \pm SEM, Comparisons between control and treated groups were analysed by using the one-way ANOVA test, $p < 0.05$ as a limit of significance.

6.3 Results

6.3.1 EECGL and WECGL suppress the *in vitro* cell proliferation of DLA cells

EECGL and WECGL inhibited DLA cell proliferation (Fig. 6.1). The IC_{50} values of EECGL and WECGL in DLA cells were 29.4 ± 0.667 , and 43.1 ± 0.978 $\mu\text{g/ml}$ respectively. The EECGL and WECGL significantly decreased DLA cell viability by 17%, 29%, 41%, 66% and 15%, 31%, 43%, 68% at 5,10, 25 and 50 mg ml^{-1} doses respectively. On the other hand, no significant reduction of lymphocyte viability was noted at the doses of EECGL and WECGL up to 50 $\mu\text{g ml}^{-1}$.

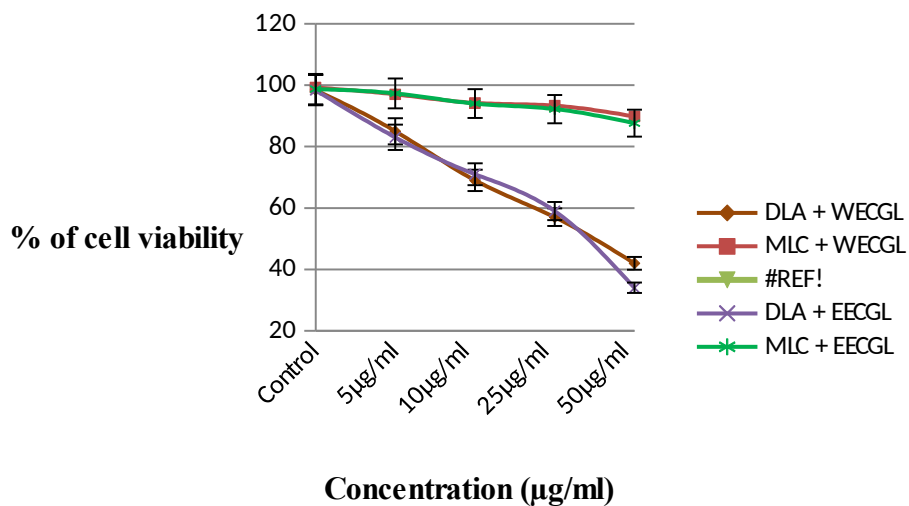


Figure 6.1 *In vitro* cytotoxic effects of EECGL and WECGL on DLA cells and MLC. Values are expressed as the Mean \pm SEM of three experiments.

6.3.2 Cellular redox status (GSH levels).

The present study showed (Fig. 6.2) decreased GSH content in EECGL and WECGL treated DLA cells significantly ($p < 0.01$ and $p < 0.05$ respectively).

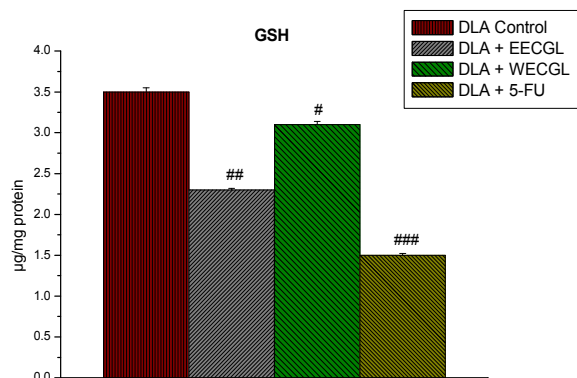


Figure 6.2 Intracellular reduced glutathione (GSH) content in EECGL and WECGL treated DLA cells. Data are expressed as Mean \pm SEM. Probability values are given in #. # indicates $p < 0.05$, ## indicates $p < 0.01$, ### indicates $p < 0.001$; values are taken in respect of control.

6.3.3 Intracellular ROS level

In DLA cell, DCF fluorescence intensity due to intracellular ROS generation was enhanced by EECGL and WECGL at their respective IC_{50} doses (Fig. 6.3). This result was correlated by respective fluorescence microscopic images.

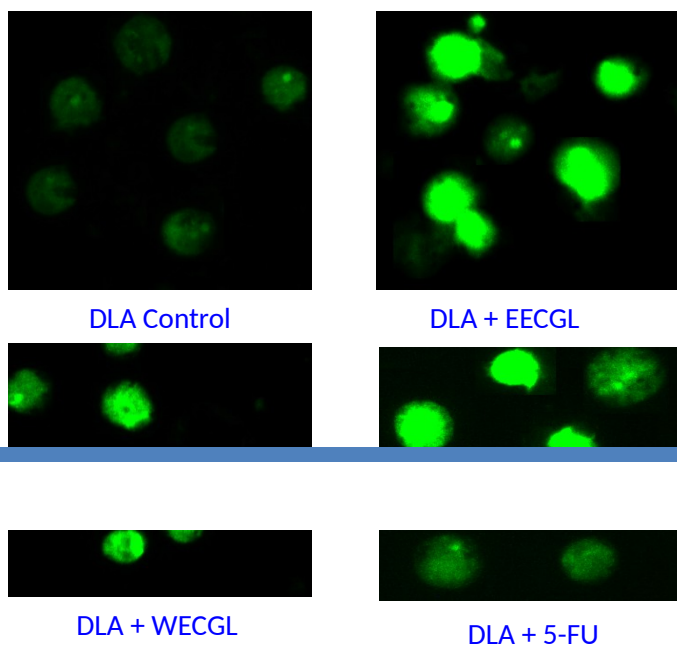


Figure 6.3. Fluorescent microscopic image of intracellular ROS generation by H₂DCFDA staining. DCF fluorescence intensity was expressed in term of ROS production. After the treatment schedule, cells were incubated with H₂DCFDA. At the end of H₂DCFDA exposure, cells were washed with phosphate-buffered saline and were visualized by fluorescence microscopy at an excitation wavelength of 485 nm and an emission wavelength of 520 nm.

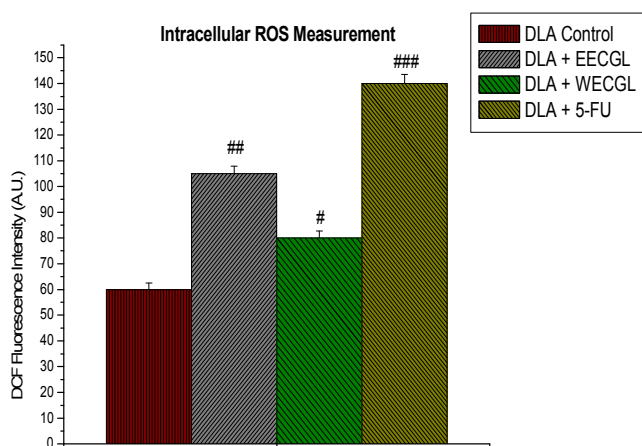


Figure 6.4 Effects of EECGL and WECGL on DCF fluorescence intensity in DLA cells.Data are expressed as Mean \pm SEM. Probability values are given in #. # indicates $p < 0.05$, ## indicates $p < 0.01$, ### indicates $p < 0.001$; values are taken in respect of control.

6.3.4 Nitric oxide (NO) release and generation level

Nitric oxide release and generation were increased in EECGL and WECGL treated DLA cells. The present study showed increased NO release in EECGL and WECGL treated DLA cells at respective significant ($p < 0.01$ and $p < 0.05$) level (Fig. 6.5 A). The NO generation level in treated DLA cell was also increased significantly ($p < 0.05$) at IC_{50} dose of EECGL (Fig. 6.5 B).

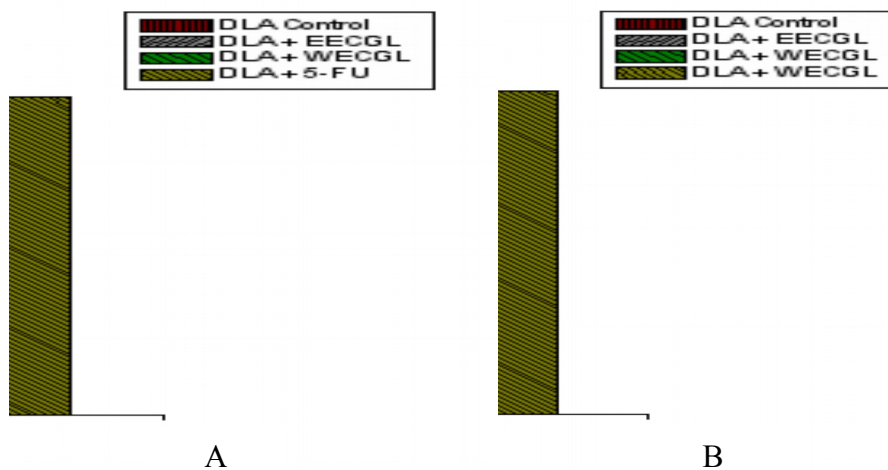


Figure 6.5 (A) Nitric oxide (NO) release and (B) NO generation levels in EECGL and WECGL treated DLA cells. Data are expressed as Mean \pm SEM. Probability values are given in asterisks. * indicates $p < 0.05$, ** indicates $p < 0.01$; values are taken in respect of control.

6.3.5 Lactate dehydrogenase (LDH) release level

LDH release was elevated in EECGL and WECGL treated DLA cells. The LDH level in DLA cell was significantly ($p < 0.05$) increased at IC_{50} dose of EECGL (Fig. 6.6).



Figure 6.6. Effects of EECGL and WECGL on LDH release level in DLA cell. Data are expressed as Mean \pm SEM. Probability values are given in asterisks. * indicates $p < 0.05$; values are taken in respect of control.

6.3.6 EECGL and WECGL induce apoptotic on DLA cells

Polarizing microscopic study confirmed the typical pattern of membrane blebbing (Fig. 6.7) induced by EECGL and WECGL as well as by reference drug 5-FU.

Chromatin condensation (Fig. 6.8) was observed under fluorescent microscope after PI and DAPI staining. Prominent chromatin condensation was seen in EECGL treated DLA cells compared to WECGL.

AO-EtBr staining showed a round and green nucleus with intact DNA containing viable cells in DLA control group. Early apoptotic cells showed fragmented DNA with yellow-colour nuclei. Late apoptotic and necrotic cell remained fragmented DNA with orange and reddish nucleus respectively. Most of EECGL and WECGL treated DLA cells showed early and late apoptotic stages after AO-EtBr staining (Fig. 6.9).

In the present study, the induction of programmed cell death was supported by DNA ladder formation by agarose gel electrophoretic study. DNA fragmentation was prominent in EECGL, WECGL and 5-FU treated DLA cells (Fig. 6.10).

Fluorescent microscopic images of mitochondrial membrane potential (MMP) in control and treated DLA cell have been shown in Fig. 6.11. Measurement of MMP was based on rhodamine 123 fluorescence intensity. The fluorescence intensity (Fig. 6.12) was decreased significantly ($p < 0.05$ and $p < 0.01$) in EECGL and WECGL treated DLA cells respectively.

DNA fragmentation in DLA cells was again confirmed by alkaline comet assay (Fig. 6.13). EECGL and WECGL increased DNA fragmentation in DLA cells. The increased percentage of tail DNA intensity was observed in EECGL, WECGL and 5-FU treated lymphoma cells (Fig. 6.14).

EECGL and WECGL induced DLA cell cycle arrest at the G_0/G_1 phase, as shown in Fig. 6.15. DNA content of treated DLA cells was analysed using PI staining, and cell distributions among sub- G_1 , G_0/G_1 , S and G_2/M phases were expressed. Cells were treated with the IC_{50} concentrations of EECGL and WECGL for 24 h. Results revealed increasing accumulation of cells at the G_0/G_1 phase over time. Accumulation of G_0/G_1 phase cells was significantly greater in cells treated with either extract than in control, corroborating the results of the MTT cell proliferation assay.

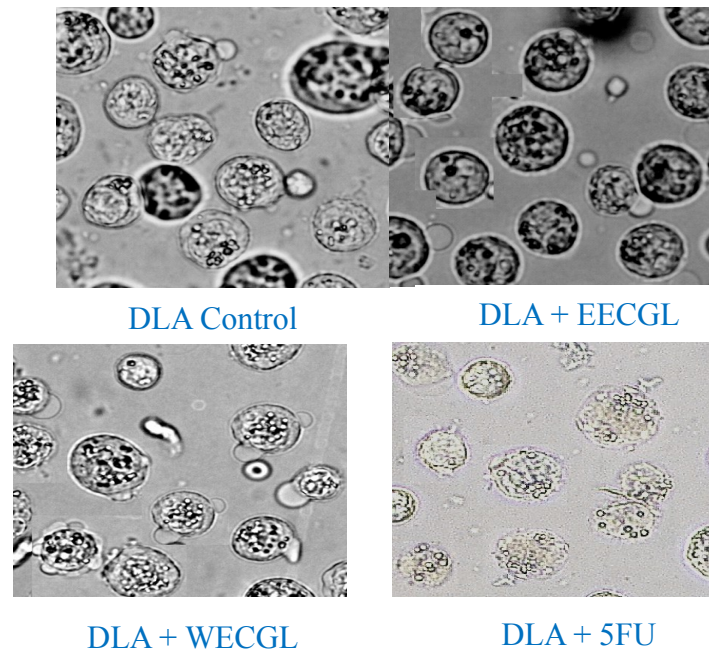


Figure 6.7.Photomicrographs of membrane DLA cells treated with EECGL and WECGL and 5-FU under polarizing microscope.

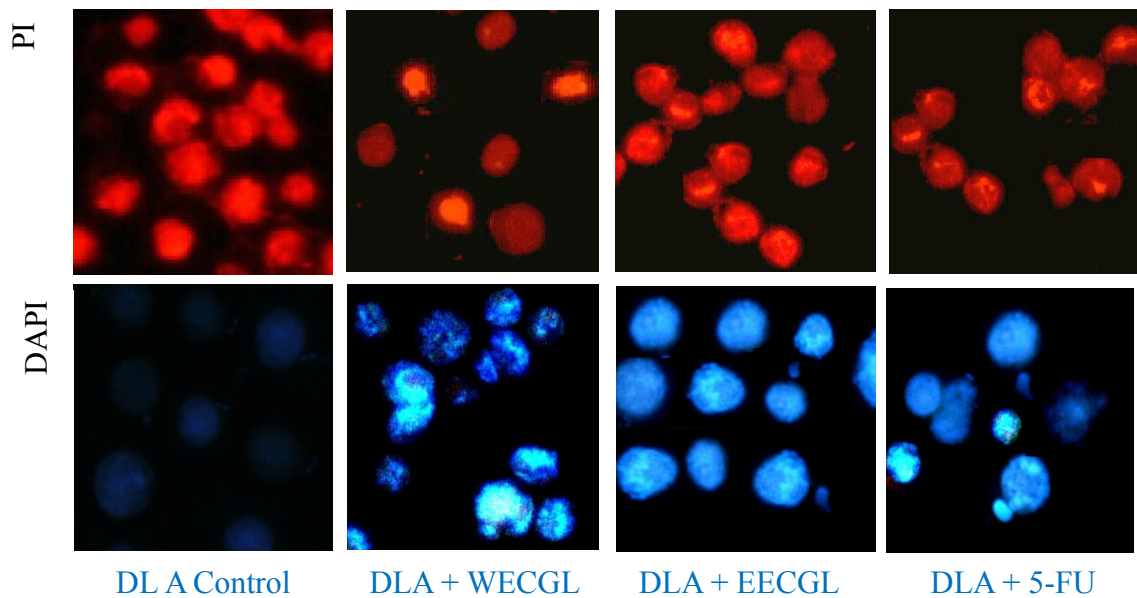


Figure 6.8. Fluorescent microscopic image of chromatin condensation in DLA cells treated with EECGL, WECGL and 5-FU along with DLA control. Cells were stained with PI and DAPI staining

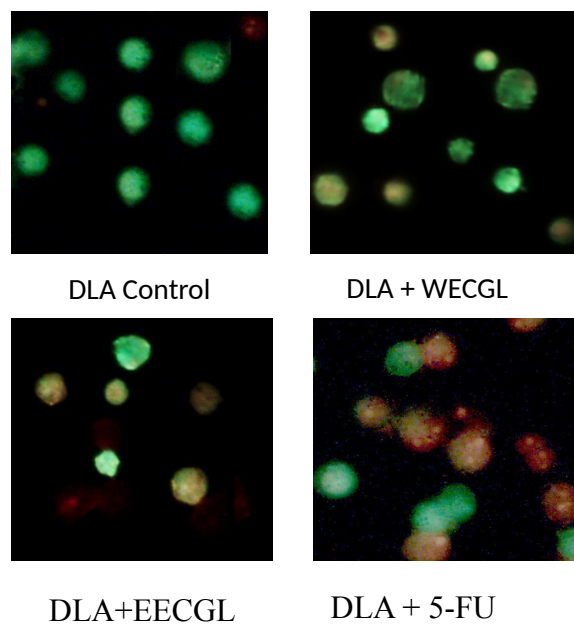


Figure 6.9 Fluorescent microscopic images of AO-EtBr stained EECGL and WECGL treated DLA cells. Staining shows a round and green nucleus with intact DNA in viable cells; early apoptotic cells show fragmented DNA with yellow-colour nuclei; late apoptotic and necrotic cell represent fragmented DNA with orange and red nucleus respectively.

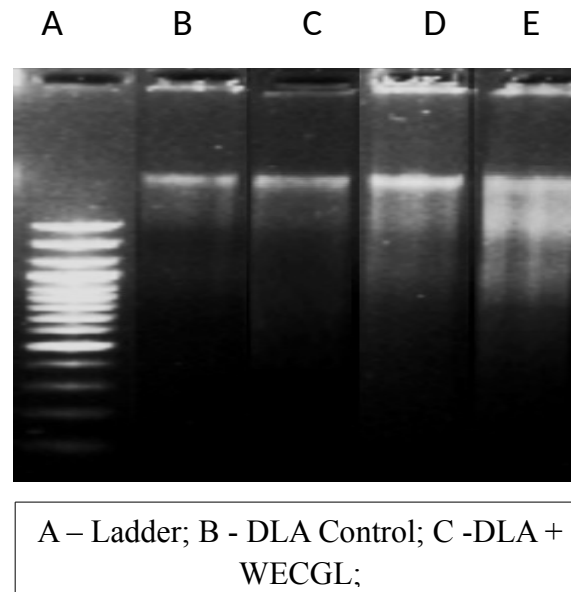


Figure 6.10 DNA laddering in EECGL and WECGL treated DLA cells.

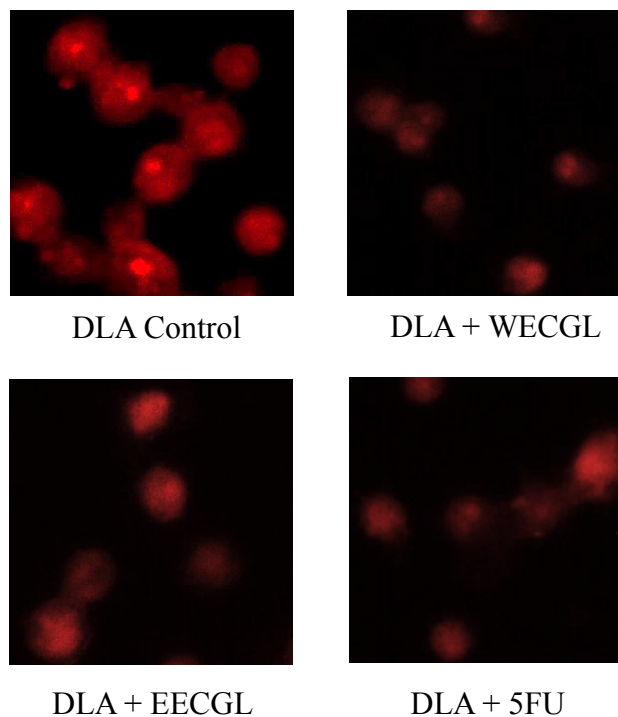


Figure 6.11 Fluorescent microscopic images of mitochondrial membrane potential in EECGL and WECGL treated DLA cells after staining with Rhodamine

123.Measurement of mitochondrial membrane potential (MMP) of DLA cell treated with EECGL and WECGL.

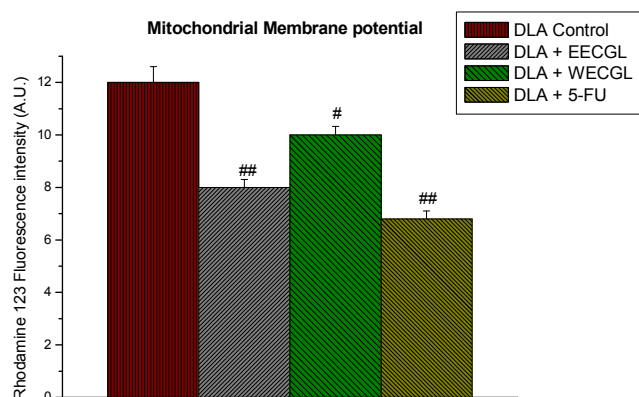
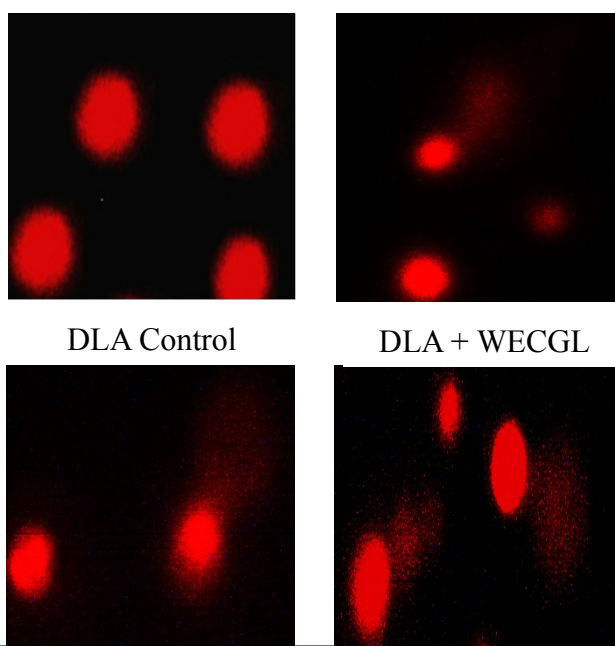


Figure 6.12 Mitochondrial membrane potential as indicated by Rhodamine 123 intensity in EECGL and WECGL treated DLA cells. Data are expressed as Mean \pm SEM. Probability values are given in #. # indicates $p < 0.05$, ## indicates $p < 0.01$; values are taken in respect of control.

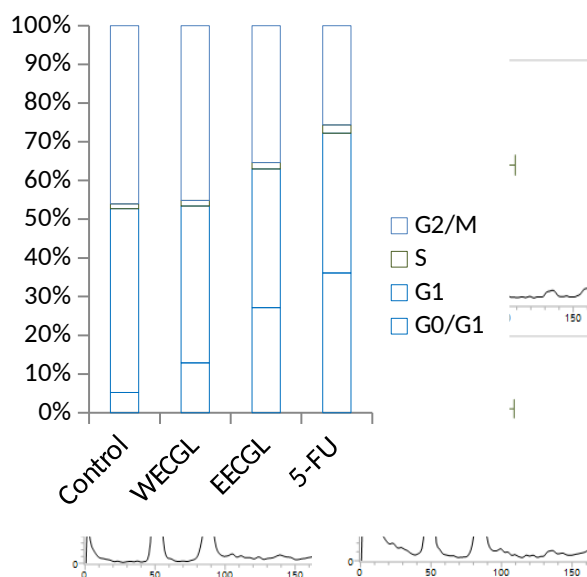


DLA + EECGL DLA + 5FU

Figure 6.13.Fluorescent microscopic image of DNA damage by alkaline comet assay in EECGL and WECGL treated DLA cells.



Figure 6.14. The percentage of tail DNA intensity in alkaline comet assay as measured in treated DLA cells. Data are expressed as Mean ± SEM. Probability values are given in asterisks. *indicates $p < 0.05$, *** indicates $p < 0.001$; values are taken in respect of control.



(A)
Figure 6.15. Flow cytometer-based apoptosis assay (B) cells were treated with respective IC_{50} of EECGL and WECGL for 24 hours, and stained with PI and measured by flow cytometry. (B) Accumulation of G_0/G_1 cells plotted from the cell cycle-based apoptosis assay. Data are presented as Mean \pm SEM from three independent experiments.

6.3.7 Effect of EECGL and WECGL on tumor growth of DLA-bearing mice

The result in Fig. 6.16 indicates that control DLA-bearing mice had a gradual increase in body weight from the day zero. When compared to the body weight of control DLA-bearing mice on day 15, the body weight of the treated mice decreased significantly by about 50%, indicating the effect of EECGL and WECGL in preventing the growth of DLA cells.

Inhibition of tumor growth in vivo expressed by the mean survival time (MST) and Increase life span (ILS) have been shown in Fig 6.17(A,B) and 6.18 (A,B). In case of DLA control, mean survival time is 14 ± 0.57 whereas with high dose of (200 mg/kg of body weight) of EECGL, mean survival time is 25 ± 0.88 days indicating 78.57% increase in longevity of the treated group with respect to DLA control. High dose (200 mg/kg of body weight) of WECGL, mean survival time is 15.33 ± 0.88 days indicating 9.5% increase in longevity of the treated group with respect to DLA control. EECGL and WECGL have demonstrated enhanced effect on the mean life span by 68% and 33%.

After treatment with EECGL and WECGL (100 and 200 mg/kg) the tumor volume of DLA induced mice was significantly reduced (Fig. 6.17). Tumor cell count (on 15th day) was also decreased after treatment with EECGL and WECGL (100 and 200 mg/kg) compared to DLA control animals (Fig. 6.22) and in both cases EECGL was more potent than WECGL.

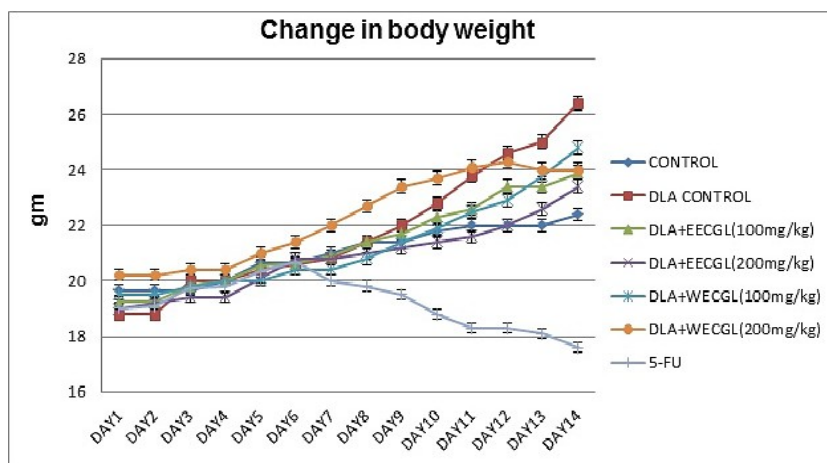


Figure 6.16. The effect of EECGL and WECGL on change of body weight in DLA bearing mice. Data are expressed as Mean± SEM.

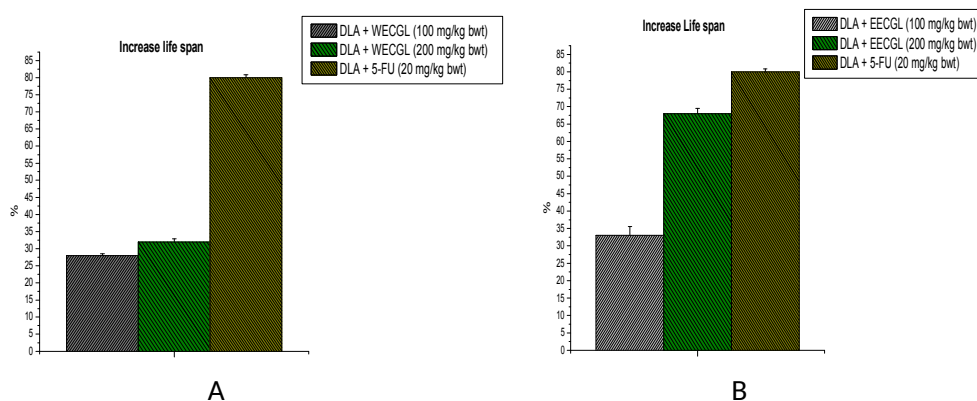


Figure 6.17. The effect of EECGL and WECGL on Increase life span (ILS) in DLA bearing mice. Data are expressed as Mean± SEM

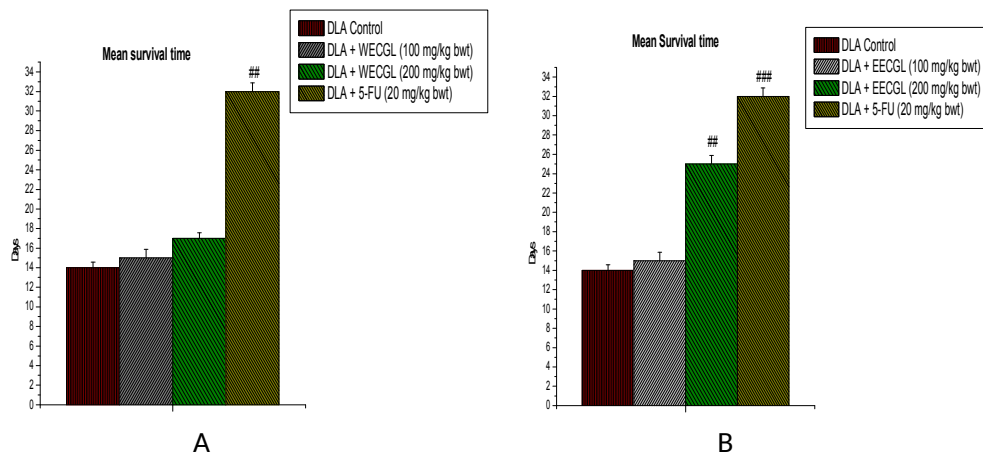


Figure 6.18. The effect of EECGL and WECGL on Mean survival time (MST) in DLA bearing mice. Data are expressed as Mean \pm SEM. Probability values are given in asterisks. ## indicates $p < 0.01$, ### indicates $p < 0.001$; values are taken in respect of DLA control.

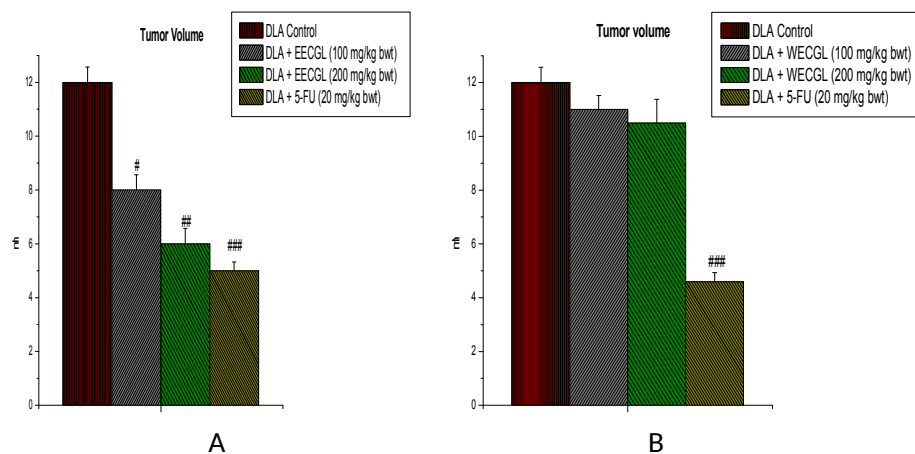


Figure 6.19. The effect of EECGL and WECGL on Tumor volume in DLA bearing mice. Data are expressed as Mean \pm SEM. Probability values are given in asterisks. #

indicates $p < 0.05$, ## indicates $p < 0.01$, ### indicates $p < 0.001$; values are taken in respect of DLA control.

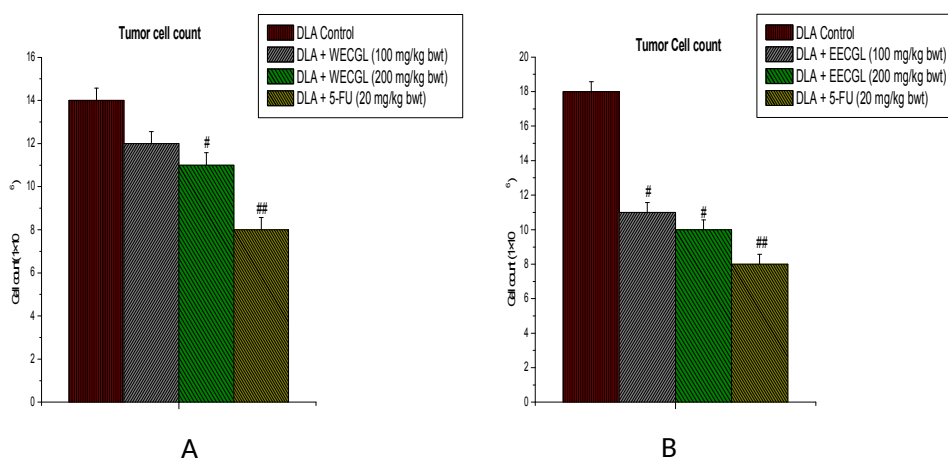


Figure 6.20. The effect of EECGL and WECGL on Tumor cell count in DLA bearing mice. Data are expressed as Mean \pm SEM. Probability values are given in asterisks. # indicates $p < 0.05$, ## indicates $p < 0.01$; values are taken in respect of DLA control.

6.3.8 Effect of EECGL and WECGL on haematological parameters

Haematological parameters of DLA-bearing mice on day 15 were found to be significantly changed from normal (saline control) group (Table 6.1 and 6.2). Haemoglobin content and RBC count in the DLA control group was significantly ($p \leq 0.001$) decreased in comparison to the normal group. EECGL and WECGL at 100 and 200 mg/kg body wt. dose levels increased the haemoglobin content and RBC counts significantly. The total WBC counts were

found to be increased significantly in the DLA control group ($p < 0.001$). Administration of EECGL and WECGL at the above said doses reduces the WBC counts.

Table 6.1 Effect of EECGL on haematological parameters on DLA bearing mice

Haematological Parameters	Saline control	DLA Control	DLA + EECGL (100mg/Kg bwt)	DLA + EECGL(200mg/Kg bwt)	DLA + 5-FU (20 mg/Kg bwt)
Hb Percentage	15±0.577	10.09±0.35**	11.82±0.23#	12.43±0.14##	13±0.29##
Total RBC Count (cu.mm)	6.23±0.145	1.92±0.06**	3.8±0.11#	4.2±0.057##	5.6±0.057##
Total WBC Count(cu.mm)	5100±58	9200±153**	8500±115#	8345±80 #	5700±88###

Table 6.2 Effect of WECGL on haematological parameters on DLA bearing mice

Haematological Parameters	Saline control	DLA Control	DLA + WECGL (100mg/Kg bwt)	DLA + WECGL(200mg/Kg bwt)	DLA + 5-FU (20 mg/Kg bwt)
Hb Percentage	15±0.577	10.09±0.35**	11.92±0.154#	12.05±0.2##	13.3±0.29##
Total RBC Count (cu.mm)	6.23±0.145	1.92±0.06**	3.3±0.032#	4.12±0.05##	5.6±0.057##
Total WBC Count(cu.mm)	5100±58	9200±153**	8500±120 #	8245±78#	5767±88###

Data are expressed as Mean ± SEM. Probability values are given in asterisks and #. ** indicates $p < 0.01$, *** indicates $p < 0.001$; values are taken in respect of saline control.#

indicates $p < 0.05$, ## indicates $p < 0.01$, ### indicates $p < 0.001$; values are taken in respect of DLA control.

6.3.9 Effect of EECGL and WECGL on antioxidant parameters

The levels of MDA were significantly ($p < 0.001$) increased in DLA control animals compared to that of normal saline control animals. After treatment with EECGL at the dose levels of 100, 200 mg/kg body wt., MDA was decreased significantly ($p < 0.05$) in kidney but in liver it was decreased significantly ($p < 0.05$) at 200 mg/kg body wt. (Fig 6.21). In case of WECGL, MDA level was reduced significantly ($p < 0.05$) in kidney at both dose levels but in liver there was no significant change compared to DLA control group.

Prominent ($p < 0.001$) decrease in liver and kidney GSH level was observed in DLA control animals. The treatment with EECGL at the dose levels of 100 and 200 mg/kg body wt. reversed GSH level to near normal values in the liver and kidney samples (Fig 6.22). Most of the results regarding GSH level were found to be significant ($p < 0.05$) those of observed with 5-FU treatment. WECGL also restored these values towards the normal status; same as at the dose level of 200 mg/kg body wt. ($p < 0.01$), decrease in the activity of liver and kidney superoxide dismutase (SOD) was observed in DLA control animals. The treatment with EECGL at 100 and 200 mg/kg body wt. doses reversed these changes to near normal values in the liver and kidney of treated mice (Fig 6.23). Almost similar results were seen in 5-FU treated mice. EECGL at 200 mg/kg body wt. dose level was found to be more potent.

WECGL at both dose levels (Fig 6.23) normalized the SOD activity to a good extent ($p < 0.01$) compared to DLA control.

The activity of catalase (CAT) was significantly ($p < 0.001$) decreased in DLA control animals compared to normal control animals. After treatment with EECGL and WECGL at 100 and 200 mg/kg body wt., CAT activity was increased significantly ($p < 0.05$) in the kidney but in the liver it increased significantly ($p < 0.05$) by EECGL at 200 mg/kg body wt. (Fig 6.24). After treatment with 100, 200 mg/kg of WECGL, CAT activity was increased significantly ($p < 0.001$) in the liver compared to DLA control.

The activity of glutathione peroxidase (GPx) was significantly ($p < 0.001$) decreased in DLA control animals when compared with normal control animals. After treatment with EECGL, GPx activity increased significantly ($p < 0.05$) in the liver but more pronouncedly ($p < 0.01$) in the kidney at 200 mg/kg dose level (Fig 6.25). In case of WECGL, GPx activity was increased significantly ($p < 0.01$) in the kidney and liver compared to DLA control at 200 mg/kg body wt. dose.

Pronounced ($p < 0.001$) decrease in liver and kidney GST activity was also seen in DLA control animals. The treatment with EECGL at the above mentioned dose levels did not show any significant changes ((Fig 6.26). After treatment with WECGL, GST activity was increased significantly ($p < 0.05$) in the kidney compared to those in DLA control group.

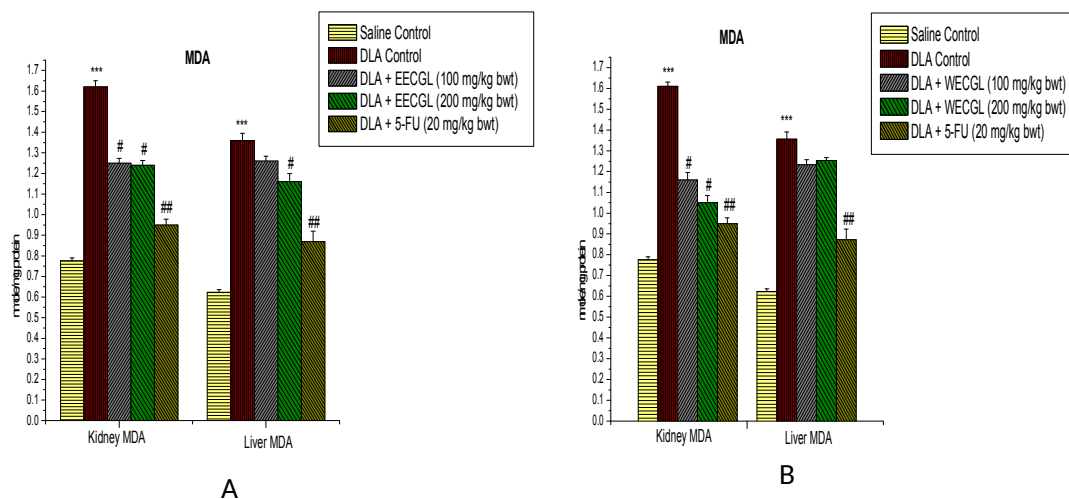


Figure 6.21. The effect of EECGL and WECGL on liver and kidney MDA in DLA bearing mice. Data are expressed as Mean± SEM. Probability values are given in asterisks and #. ‘***’ represents significant difference at ($p < 0.001$) compared to saline control; # indicates $p < 0.05$, ## indicates $p < 0.01$; values are taken in respect of DLA control.

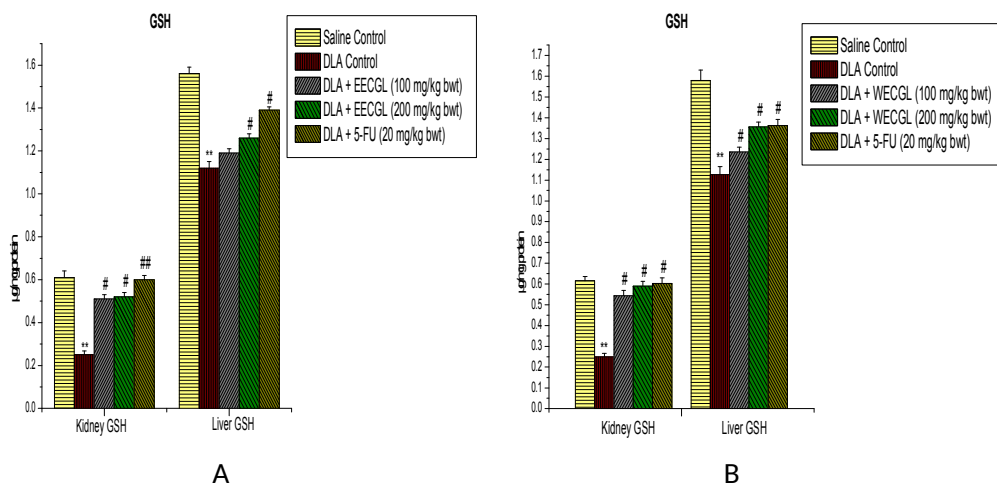
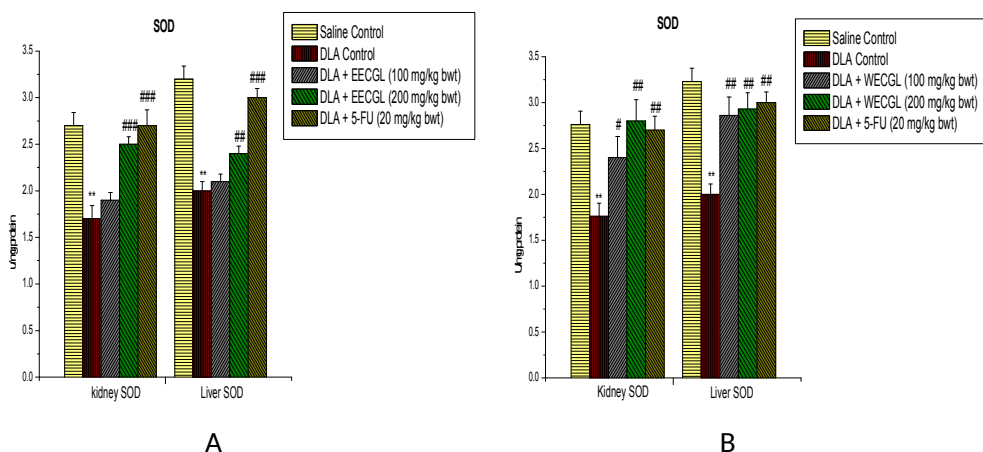


Figure 6.22. Liver and kidney GSH in DLA bearing mice after the treatment of EECGL and WECGL. Data are expressed as Mean \pm SEM. Probability values are given in asterisks and #. ‘**’ represents significant difference at ($p < 0.001$) compared to saline control; # indicates $p < 0.05$, ## indicates $p < 0.01$; values are taken in respect of control.



bearing mice. Data are expressed as Mean \pm SEM. Probability values are given in asterisks and #. ** indicates $p < 0.01$; values are taken in respect of saline control. # indicates $p < 0.05$, ## indicates $p < 0.01$, ### indicates $p < 0.001$; values are taken in respect of DLA control.

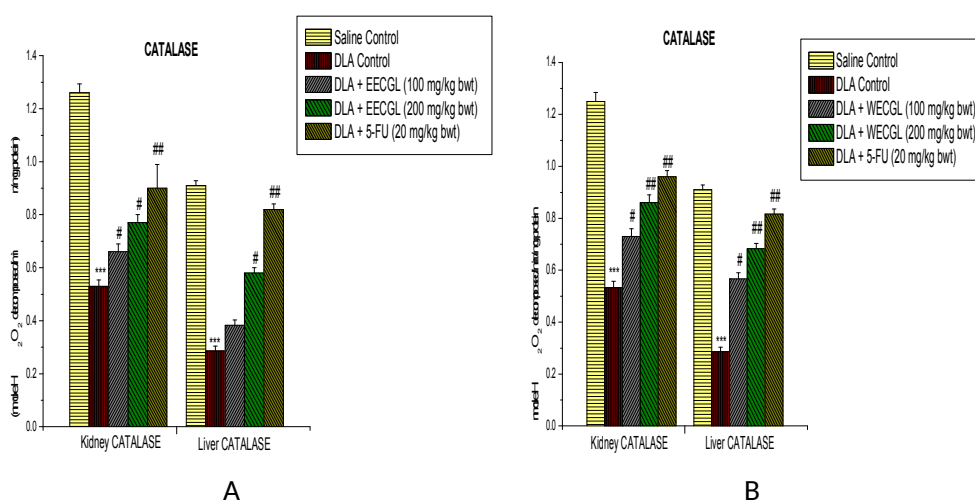


Figure 6.24. Liver and kidney catalase in DLA bearing mice after the treatment of EECGL and WECGL. Data are expressed as Mean \pm SEM. Probability values are given in asterisks and #. ** indicates $p < 0.01$, *** indicates $p < 0.001$; values are taken in respect of saline control. # indicates $p < 0.05$, ## indicates $p < 0.01$; values are taken in respect of DLA control

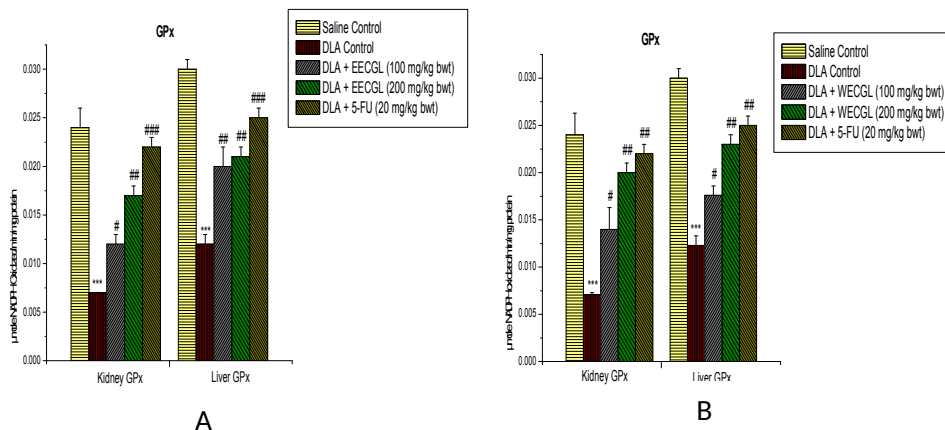


Figure 6.25. The effect of EECGL and WECGL on liver and kidney GPx in DLA bearing mice. Data are expressed as Mean \pm SEM. Probability values are given in asterisks and #. *** indicates $p < 0.001$; values are taken in respect of saline control. # indicates $p < 0.05$, ## indicates $p < 0.01$, ### indicates $p < 0.001$; values are taken in respect of DLA control.

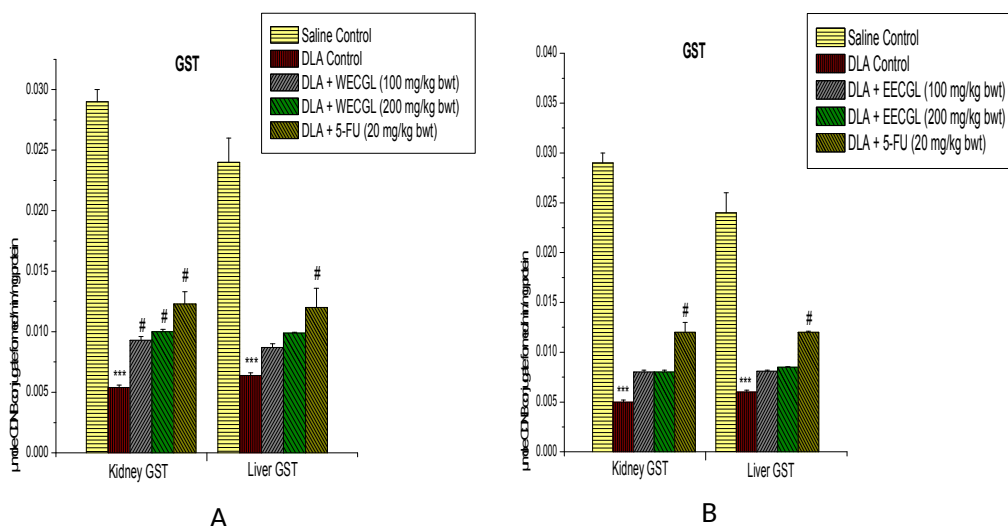


Figure 6.26. Liver and kidney GST in DLA bearing mice after the treatment of EECGL and WECGL. Data are expressed as Mean \pm SEM. Probability values are given in asterisks and #. *** indicates $p < 0.001$; values are taken in respect of saline control. # indicates $p < 0.05$; values are taken in respect of DLA control.

6.4 Discussion

The present chapter deals with the evaluation of the cytotoxic, apoptotic, antioxidant and antiproliferative potential of ethanol (EECGL) and water (WECGL) extract of *Calotropis gigantea* latex against Dalton's ascites lymphoma (DLA) cells *in vitro* and *in vivo* experimental conditions.

EECGL and WECGL exert their *in vitro* cytotoxic effects against DLA cells showing IC_{50} values of 29.4 and 43.1 $\mu\text{g/ml}$ respectively.

Reduced glutathione is an important intracellular reductant and offers protection against free radicals and toxic agents. In different pathological conditions and diseases cellular GSH concentrations are depleted by oxidation of GSH to GSSG and this conversion is caused by oxidative stress (Gravila et al., 2010). Decreased levels of DLA intracellular GSH might be a result of the effective conversion of GSH to GSSG by increased free radicals in DLA cells induced by EECGL and WECGL. It demonstrates the anticancer potential of EECGL and WECGL, which was further confirmed by other *in vitro* and *in vivo* experiments including FACS analysis. Similarly, the results indicate that a significant ($p < 0.01$) increase of

ROS level is found due to EECGL and WECGL exposure (Fig. 6.4). The fluorescence images are highly correlated with the fluorescence intensity level. ROS are such natural by-products which contain unpaired valence electrons, being highly active and have a specific role in cell signaling and homeostasis of cell environment (Sena and Chandel,2012) leading to oxidative damage. Intracellular ROS generation mainly caused by mitochondrial respiratory chain reaction and membrane bound superoxide-generating enzyme i.e., nicotinamide adenine dinucleotide phosphate (NADPH) oxidase mediated reactions (Pereira et al., 2012).In this study, EECGL and WECGL may interrupt mitochondrial membrane integrity of DLA cell, evidenced by MTT assay. The impairment of mitochondrial electron transport chains may elevate ROS generation (Jeyaraj et al.,2013). Again elevated levels of ROS may stimulate the release of different pro-inflammatory markers such as TNF- α . TNF- α activates nuclear factor-kB and last of all leads to cell death by apoptotic and necrotic pathways (Shen and Pervaiz, 2006). In a biological system, the free radical NO is an intra- and inter-cellular messenger (Jaffrey & Snyder, 1995). NO reacts with superoxide to form more toxic peroxynitrite (ONOO), which has important tumoricidal functions. The excess production of NO shows massive oxidative injury. In the study, a higher level of nitrite was released and generated in EECGL and WECGL-treated lymphoma cells owing to the high production of free radicals, mainly NO.

To investigate the anticancer mechanism of EECGL and WECGL, the cytotoxicity was assessed using the LDH release assay. EECGL and WECGL were found to disrupt the membrane integrity of the lymphoma cells and thereby increase LDH release.

Occurrence of membrane blebbing and bluish/orange condensed chromatin in DLA cells after treatment with EECGL and WECGL at IC_{50} doses clearly indicated the apoptotic properties of EECGL and WECGL in DLA cells. Fluorescence microscopic image of EAC cells stained by PI and DAPI confirmed that EECGL and WECGL have the ability to inhibit the cell proliferation via apoptosis. Treatment of EECGL and WECGL exhibited typical apoptotic morphology (Fig. 6.8) with condensed nuclei in treated DLA cell compared to DLA control. As membrane integrity became compromised and PI and DAPI stain leaked into intact membrane, even in shrunken cell, the apoptotic nuclei appeared bright pink chromatin and bright blue chromatin that are highly condensed and fragmented (Bortner and Cidlowski, 1998). Acridine orange/ethidium bromide staining in this study indicated that EECGL and WECGL primarily induced apoptosis in the cancer cells. The subsequent study was done to understand the underlying molecular mechanism of EECGL and WECGL on DLA cell, which revealed that EECGL and WECGL induce apoptosis in DLA cells by activation of caspase cascade and DNA fragmentation. Depletion of mitochondrial membrane potential is another marker of apoptosis-induced cell death (Adrie et al., 2001). The present study showed that an effective dose of EECGL and WECGL decreased mitochondrial membrane potential as compared to DLA control. Alteration of mitochondrial membrane potential in extracts treated lymphoma cells may result in malfunction in ATP synthesis and maintenance of the ATP level that leads to either apoptosis or necrosis. Apoptosis does not depend only on depleted ATP synthesis, whereas a decreased level of ATP ensures apoptosis induction (Yang

and Schaich, 1996). The increase in the tail DNA (%) can be as a result of direct induction of DNA strand breaks or disruption of DNA backbones by compounds or its byproducts, such as free radicals (Yang and Schaich, 1996). The induction of apoptosis was confirmed through flow cytometry after PI staining in this study, in which EECGL and WECGL caused an increase in the percentage of apoptotic cells with a G₀/G₁phase. Cell arrest at the G₀/G₁phase is a typical characteristics exhibited by cells that are undergoing apoptosis. Several phytochemicals have been reported to inhibit the growth of cancer cells through cell cycle arrest (Aggarwal et al., 2004). In the present study it was found that EECGL and WECGL could induce G₀/G₁phase arrest in DLA cells (Loganayaki and Manian, 2012).

We further confirmed the anticancer activity of *C. gigantea* latex by the treatment of EECGL and WECGL in DLA bearing mice. The weight of the DLA induced mice gradually increases with passage of time due to accumulation of ascitic fluid in the abdomen. Hence change in weight is considered as a parameter to determine the intensity of the disease. EECGL and WECGL at 200 mg/kg caused significant decrease in body weight of the animal, while in the untreated group of animals the increase in weight was about 35 g. More interestingly, it was found that the DLA bearing mice administered with 100 mg/kg and 200 mg/kg of EECGL prolonged the life span of the animals significantly than WECGL. In Dalton's lymphoma bearing mice peritoneal fluid is the direct nutritional source for tumor cells (Prasad and Giri, 1994). Treatment with EECGL significantly reduced the tumour volume probably by lowering the ascitic fluid volume. Decrease in DLA cell count in EECGL and WECGL

treated group of animals indicates that the test extracts are having *in vivo* antiproliferative activity on DLA cells.

In the tumor control group marked increase in WBC count and decrease in RBC count was observed. Interestingly, it was found from our results that treatment with EECGL and WECGL extract could restore the haematological parameters in the treated groups. In this case it can be postulated that due to progression of cancer, WBC levels increased in the DLA induced animals. On treatment with the EECGL and WECGL, the WBC and RBC levels were significantly restored. It was observed that the level of WBC severely raised up for the DLA induced untreated group of animals whereas the RBC count and hemoglobin count of these group drastically dropped down as compared to normal animals.

MDA is the end product of lipid peroxidation and present in the carcinomatous tissue at higher concentration than normal tissue (Yagi, 1991). In this experiment it is noted that treatment with EECGL decreased the levels of lipid peroxidation in DLA bearing mice. So, it is clear that EECGL have antioxidant activity. Reduced glutathione (GSH) shows a key role in cell defense mechanisms by acting as an antioxidant or by reacting with many toxic agents to form conjugates that are eliminated from the cell (Deleve and Kaplowitz, 1991). Cancer cells can produce large amounts of hydrogen peroxide that may be capable to damage normal tissues (Szatrowski and Nathan, 1991). The observed depletion of GSH level in the DLA bearing mice cells may suggest its involvement in the scavenging of excess free radicals in tumor cells.

In cancer, a large amount of reactive oxygen species is generated. It has been demonstrated that antioxidant enzyme levels are low in most animal and human cancers. Catalase (CAT) was also decreased in the animals in DLA control group and was increased significantly in extract treated group. During oxidative stress detoxification pathways is triggered and involvement of multiple antioxidant enzymes occurs. Superoxide dismutase (SOD) catalyzes the first step and then CAT and various peroxidases removes hydrogen peroxide from cell in order to prevent the formation of free radicals. These enzymes protect DNA from oxidative stress and prevent the individual's risk of cancer susceptibility (Elaine et al.,2012). A reduction of peroxidase enzyme level in DLA control group was seen which was tend to be normalized by extract treatment. SOD plays an important role in the antioxidant enzyme defense system by converting superoxide radicals into hydrogen peroxide (Devasagayam et al., 2004). EECGL and WECGL enhanced the activity of SOD in mice in our study. Therefore our study revealed that increased levels of SOD and CAT showed protective effects on liver and kidney from cancer induced oxidative stress. Plant derived extracts comprising antioxidant principles showed antitumor activity in experimental animals (Marklund et al.,1982). The role of free radicals in cancer is well documented (Putul et al., 2000; Ravid and Korean,2003). The lowering of lipid peroxidation, GST, GPx and increasing of SOD and catalase levels in EECGL and WECGL treated groups indicates its potential as an inhibitor of DLA induced intracellular oxidative stress.

6.5 Conclusion

In conclusion, the findings demonstrate that ethanol (EECGL) and water (WECGL) extracts of *Calotropis gigantea* latex display anticancer activity in DLA cells. *In vitro* analysis by the ROS generation, LDH release assay, mitochondrial membrane potential measurement, flow cytometric analysis, and acridine orange/ethidium bromide staining indicated that EECGL and WECGL primarily induced apoptosis in the DLA cells. The present study established that the latex extracts increased the life span of DLA bearing mice and it enhanced the antioxidant status and reduced the lipid peroxidation. It is proved that the plant can be exploited as a source of novel drug development for cancer treatment. Further investigations are needed to elucidate the antitumor activities of exact compounds, which are present in this plant latex.

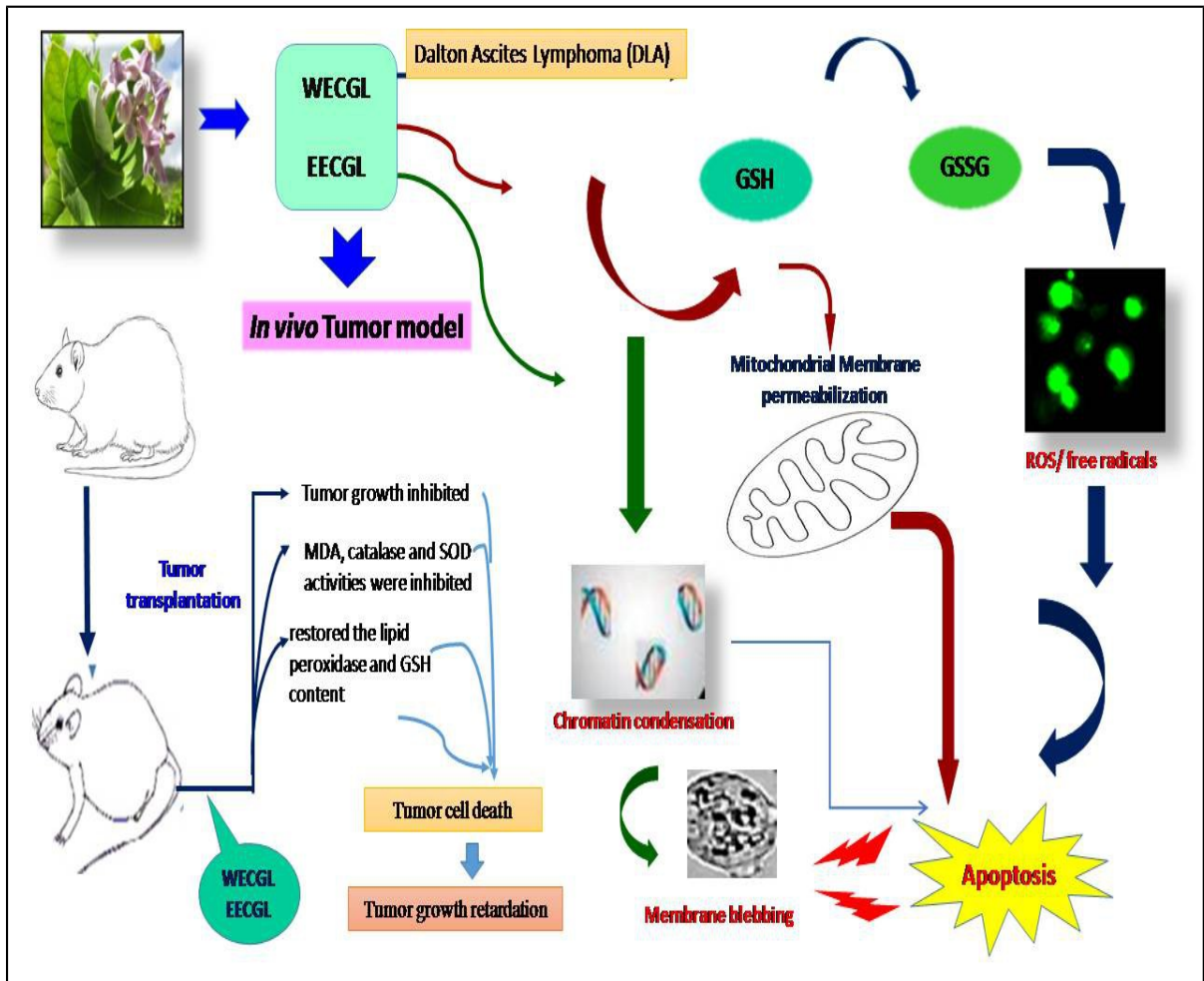


Figure 6.27 Mechanistic view of anticancer activity of *Calotropis gigantea* latex

|

6.6 References

Adrie C, Bachelet M, Vayssier-Taussat M, Russo-Marie F, Bouchaert I, Adib-Conquy M, Cavaillon JM, Pinsky MR, Dhainaut JF, Polla BS. Mitochondrial membrane potential and apoptosis peripheral blood monocytes in severe human sepsis. *2001; American Journal of Respiratory and Critical Care Medicine*. 2001; 164:389–395.

Aebi H. Catalase. In: Bergmeyer H.U., editor. *Methods of Enzymatic Analysis*. Academic Press; New York, NY, USA; 1974. p. 673–677.

[Aggarwal BB](#), [Bhardwaj A](#), [Aggarwal RS](#), [Seeram NP](#), [Shishodia S](#), [Takada Y](#) Role of resveratrol in prevention and therapy of cancer: preclinical and clinical studies. *Anticancer Research*. 2004 ;24:2783-840.

Alcântara DD, Ribeiro HF, Cardoso PC, Araújo TM, Burbano RR, Guimarães AC, Khayat AS, Oliveira BM. In vitro evaluation of the cytotoxic and genotoxic effects of artemether, an antimalarial drug, in a gastric cancer cell line (PG100). *Journal of Applied Toxicology*. 2011; 33:151–156.

Al-Qubaisi M, Rozita R, Yeap SK. Selective cytotoxicity of goniothalamin against hepatoblastoma hepg2 cells. *Molecules*. 2011; 16:2944-59.

Bala A, Kar B, Haldar PK, Mazumder UK, Bera S. Evaluation of anticancer activity of *Cleome gynandra* on Ehrlich's Ascites Carcinoma treated mice. *Journal of Ethnopharmacology*.2010; 129:131–134.

[Bortner CD](#), [Cidlowski JA](#). A necessary role for cell shrinkage in apoptosis. *Bochemcal Pharmacology*.1998; 56:1549-59.

Chakraborty SP, Mahapatra SK, Sahu SK, Das S, Tripathy S, Dash S, Pramanik P, Roy S. Internalization of staphylococcus aureus in lymphocytes induces oxidative stress and dna fragmentation: possible ameliorative role of nanoconjugatedvancomycin. *Oxidative Medicine and Cellular Longevity*. 2011; 2011: 942123.

Coustan-Smith Elaine, Charles G. Mullighan, OnciuMihaela,. Behm Prof. Frederick G,Raimondi Prof. Susana C,Pei Deqing , Cheng Cheng, Xiaoping Su, Jeffrey E. Rubnitz, Basso Prof. Giuseppe, Biondi Prof. Andrea, Pui Prof. Ching-Hon, Downing Prof. James R., Campana Prof. Dario. Early t-cell precursor leukemia: a subtype of very high-risk acute lymphoblastic leukemia identified in two independent cohorts. *The Lancet Oncology*. 2009 ; 10: 147–156.

Dacie JV, Lewis SM. *Practical hematology*. 2nd ed. London: J and A Churchill; 1958. p. 38–48.

Deleve LG, Kaplowitz N. Glutathione metabolism and its role in hepatotoxicity. *Pharmacol ogy and Therapeutic*.1991; 52: 287-305.

- Devasagayam TPA, Tilak JC, Bolor KK, Sane Ketaki S, Ghaskadbi Saroj S, Lele RD. Free Radicals and Antioxidants in Human Health: Current Status and Future Prospects. *Journal of the Association of Physicians of India*. 2004; 52: 794-804.
- Dewade DR, Christina AJM, Chidambaranathan N, Bhajipale NS, Tekade NP. Antitumor activity of *Vitex negundo* linn. against Dalton's ascitic lymphoma *International Journal of PharmTech Research*. 2010; 2:1101-1104.
- Elaine HW, Jesus M, Ivan LC. Role of lipid peroxidation and antioxidant enzymes in omega 3 fatty acids induced suppression of breast cancer xenograft growth in mice. *Cancer Cell International*. 2002; 2: 10: 1-9.
- Gisselbrecht C, Gaulard P, Lepage E, Coiffier B, Briere J, Haioun C, Cazals-Hatem D, Bosly A, Xerri L, Tilly H, Berger F, Bouhabdallah R, Diebold J. Prognostic significance of T-cell phenotype in aggressive non-Hodgkin's lymphomas. *Grouped'Etudes des Lymphomes de l'Adulte (GELA)*. *Blood*. 1998; 92:76–82.
- Gong J, Traganos F, Darzynkiewicz Z. A selective procedure for DNA extraction from apoptotic cells applicable for gel electrophoresis and flow cytometry. *Analytical Biochemistry*. 1994; 218:314–319.
- Grăvilă C, Petrovici S, Stana L, Olariu L, Trif A. Study on the blood glutathione protective effects induced during three rats generations by K₂Cr₂O₇ intake. *Journal of Agroalimentary Processes and Technologies*. 2010; 16:313–316.

- Griffith OW. Glutathione turnover in human erythrocytes. *The Journal of Biochemistry*.1981; 256:4900-4904.
- Gupta M, Mazumder UK, Kumar RS, Kumar Thangavel S. Antitumor activity and antioxidant role of *Bauhinia racemosa* against Ehrlich ascites carcinoma in Swiss albino mice. *Acta Pharmacologica Sinica*. 2004; 25: 1070-1076.
- Habib MR, Karim MR. Effect of anhydrosophoradiol-3-acetate of *Calotropis gigantea* (Linn.) flower as antitumor agent against Ehrlich's ascites carcinoma in mice. *Pharmacology Reports*.2013; 65:761–767.
- Habig WH, Pabst MJ, Jakoby WB. Glutathione-S-Transferase: the first enzymatic step in mercapturic acid formation. *The Journal of Biochemistry*.1974; 249:7130–7139.
- Haldar PK, Kar B, Bala A, Bhattacharya S, Mazumder UK. Antitumor activity of *Sansevieria roxburghiana* rhizome against Ehrlich's ascites carcinoma in mice. *Pharmaceutical Biology* .2010;48: 1337.
- Ho K, Yazan LS, Ismail N, Ismail M. Apoptosis and cell cycle arrest of human colorectal cancer cell line HT-29 induced by vanillin. *Cancer Epidemiology*. 2009; 33:155–160.
- Hudson L, Hay F. *Practical Immunology*, 3rd Ed. Blackwell, Oxford; 1989.
- Jacob L, Latha MS. Anticancer activity of *Clitoria ternate* Linn. against Dalton's lymphoma. *Journal of Pharmacognosy and Phytochemical Research* .2013; 4:207-212.

- Jeyaraj R, Tamilselvam K, Manivasagam T, Namasivayam E. Neuroprotective Effect of CNB-001, a Novel pyrazole derivative of curcumin on biochemical and apoptotic markers against rotenone-induced sk-n-sh cellular model of parkinson's disease. *Journal of Molecular Neuroscience*. 2013; 22.
- Kulathuranpillai K, Narayanan N, Chidambaranathan N, Mohamed HM, Jayaprakash S. Antitumor activity of ethanolic extract of *Cnidocolus chayamansa* research article mcvaugh against dalton's ascitic lymphoma in mice. *International Journal of Pharmacy and Pharmaceutical Sciences*. 2012; 4:4.
- Li YX, Yao B, Jin J. Radiotherapy as primary treatment for stage IE and IIE nasal natural killer/T-cell lymphoma. *Journal of Clinical Oncology*. 2006; 24:181-9.
- Loganayaki N, Siddhuraju P, Manian S. Antioxidant, anti-inflammatory and anti-nociceptive effects of *Ammannia baccifera L.* (Lythraceae), a folklore medicinal plant. *Journal of Ethnopharmacology*. 2012; 140:230-3.
- M'Bemba-Meka P, Lemieux N, Chakrabarti SK. Role of oxidative stress, mitochondrial membrane potential, and calcium homeostasis in nickel subsulfide-induced human lymphocyte death in vitro. *Science of the Total Environment*. 2006; 369:21-34.
- Maiti Choudhury S, Gupta M, Majumder UK. Antineoplastic activities of MT81 and its structural analogue in Ehrlich ascites carcinoma-bearing Swiss albino mice. *Oxidative Medicine and Cellular Longevity*. 2010; 3: 61-70.

- Malik I. MD. Top 8 warning signs of lymphoma. (On line); Available from; <http://www.About.com>. 2007 .
- Marklund S, Marklund G. Involvement of superoxide anion radical in the auto oxidation of pyrogallol and a convenient assay for superoxide dismutase. *European Journal of Biochemistry*.1974; 47:469-474.
- Marklund SL, Westman NG, Lundgren E, Roos G. Copper- and zinc-containing superoxide dismutase, manganese-containing superoxide dismutase, catalase and glutathione peroxidase in normal and neoplastic human cell lines and normal human tissues. *Cancer Research*.1982; 42: 1955-1961.
- Mosmann T. Rapid colorimetric assay for cellular growth and survival: Application to proliferation and cytotoxicity assays. *Journal of Immunological Methods*. 1983; 65:55-63.
- MuthuIrulappan Sriram, Selvaraj Barath Mani Kanth, KalimuthuKalishwaralal, and SangiliyandiGurunathanAntitumor activity of silver nanoparticles in Dalton's lymphoma ascites tumor model *Internatonal Journal of Nanomedicine*. 2010; 5: 753–762.
- Nunez R. DNA Measurement and Cell Cycle Analysis by Flow Cytometry. *Current Issues of Moleculer Biology*. 2001; 3:67–70.
- Ohkawa H, Onishi N, Yagi K. Assay for lipid per-oxidation in animal tissue by thiobarbituric acid reaction. *Analytical Biochemistry*.1979; 95:351-358.

- Prasad SB, Giri A. Antitumor effect of cisplatin against murine ascites Dalton's lymphoma. *Indian Journal of Experimental Biology*. 1994;32(3):155-62.
- Prasad R, Koch B. Antitumor activity of ethanolic extract of *Dendrobium formosum* in t-cell lymphoma: an *in vitro* and *in vivo* study. *BioMed Research International*. 2014 ; 753451:11 .
- PriyaR, Ilavenil S, Kaleeswaran B, Sriganesh S, Ravikumar S. Effect of *Lawsonia inermis* on tumor expression induced by Dalton's lymphoma ascites in Swiss albino mice. *Saudi Journal of Biological Sciences*. 2011; 18:353–359.
- Putul M, Sunit C, Pritha B, Neovascularisation offers a new perspective to glutamine –related therapy. *Indian Journal of Experimental Biology*. 2000; 38:88-90.
- Ravid A, Korean R. The role of reactive oxygen species in the anticancer activity of vitamin D. *Anticancer Research*. 2003;164:357-367.
- Rotruck JT, Pope AL, Ganther HC, Hafeman DG, Hoekstro WG. Selenium: Biochemical role as a component of glutathione peroxidase. *Science*. 1973; 179:588–90.
- Roy A, Ganguly S, Bose Dasgupta BD, Pal BC, Jaisankar P Majumder HK. Mitochondria-dependent reactive oxygen species-mediated programmed cell death induced by 3,3'-diindolylmethane through inhibition of F0F1-ATP synthase in unicellular protozoan parasite *Leishmania donovani*. *Molecular Pharmacology*. 2008;74:1292–1307.

Saha P, Mazumder UK, Haldar PK, Naskar S, Kundu S, Bala S, Kar B. Anticancer activity of methanol extract of *Cucurbita maxima* against Ehrlich ascites carcinoma. International Journal of Research in Pharmaceutical Sciences. 2011; 2:52-59.

Sena LA, Chandel NS. Physiological roles of mitochondrial reactive oxygen species. Molecular Cell. 2012;48:158-67.

Shen HM, Pervaiz S. TNF receptor superfamily-induced cell death: redox-dependent execution. The FASEB Journal. 2006; 20:1589-98.

State of Healthcare in India - Lymphoma Coalition, www.lymphomacoalition.org/121uncategorised/438-state-of-healthcare-in-india. 2015.

Swerdlow SH, Campo E, Harris NL. Editors. WHO classification of tumours of haematopoietic and lymphoid tissues. In: Bosman FT, Jaffe ES, Lakhani SR, Ohgaki H, eds. World Health Organization Classification of Tumours. Lyon, France: IARC; 2008.

Szatrowski TP, Nathan CF. Production of large amounts of hydrogen peroxide by human tumor cells. Cancer Research. 1991; 51: 794-8.

Wintrobe MM. Clinical Hematology, Sixth ed. Philadelphia, USA: Lea and Febiger; 1967.

Yagi K. Lipid peroxides and human diseases. *Chemistry and Physiology of Lipids*. 1991; 45:337-351.

[Yang MH](#), [Schaich KM](#). Factors affecting DNA damage caused by lipid hydroperoxides and aldehydes. *Free Radical Biology and Medicine*. 1996; 20:225-36.

Yoganarasimhan SN. *Medicinal plants of India, Vol. I – Karnataka*. Interline Publishing Pvt., Ltd., Bangalore, India. 1996. pp. 385- 386.

